Letter

Poisson-Dirichlet distributions and weakly first-order spin-nematic phase transitions

Nils Caci ,[1] Peter Mühlbacher,[2] Daniel Ueltschi ,[2] and Stefan Wessel [1]
[1] *Institute for Theoretical Solid State Physics, JARA FIT and JARA CSD, RWTH Aachen University, 52056 Aachen, Germany*
[2] *Department of Mathematics, University of Warwick, Coventry CV4 7AL, United Kingdom*

(Received 15 September 2022; accepted 18 January 2023; published 25 January 2023)

We provide a quantitative characterization of generic weakly first-order thermal phase transitions out of planar spin-nematic states in three-dimensional spin-one quantum magnets, based on calculations using Poisson-Dirichlet distributions (PDs) within a universal loop model formulation, combined with large-scale quantum Monte Carlo calculations. In contrast to earlier claims, the thermal melting of the nematic state is not continuous, instead a weakly first-order transition is identified from both thermal properties and the distribution of the nematic order parameter. Furthermore, based on PD calculations, we obtain exact results for the order parameter distribution and Binder cumulants at the discontinuous melting transition. Our findings establish the thermal melting of planar spin-nematic states as a generic platform for quantitative approaches to weakly first-order phase transitions in quantum systems with a continuous SU(2) internal symmetry.

DOI: 10.1103/PhysRevB.107.L020409

The theory of phase transitions is fundamental to modern approaches to many-body systems and quantum matter. In particular, continuous phase transitions are a central topic in various areas of physics in view of the universality of critical phenomena. More recently, also weakly first-order phase transitions, i.e., discontinuous phase transitions with correlation lengths well beyond the lattice scale, became a topical subject in condensed matter research and beyond [1–9]. Different renormalization group (RG) scenarios explain the emergence of quasiscaling near weakly first-order phase transitions: In the "tuning" mechanism, the RG flow passes near a real infrared fixed point in theory space; in the case of "walking," the RG flow passes between two fixed points at complex couplings, associated with the collapse of two real fixed points [1,4]. An example, for which the latter scenario can be demonstrated explicitly, is the q-state Potts model with a discrete Z_q symmetry, featuring weakly first-order transitions for $q > 4$ in two dimensions [5,10–12]. Similar ideas relate to the hierarchy generation in four-dimensional gauge theories of high-energy physics within the framework of walking as a slowly running coupling constant at intermediate-energy scales [4,13–15].

For quantum many-body systems weakly first-order transitions are also central to some recently proposed interpretations of the deconfined quantum criticality (DQC) scenario [16–20] in terms of walking, fixed-point annihilation, and complex fixed points [2,3,21,22]: For DQC, quantum many-body systems are considered with continuous internal symmetries, such as U(1) or spin SU(2), for which the anticipated DQC points separate ordered regions with noncompatible symmetry-breaking patterns. The debate is still ongoing, regarding the true nature of the quantum phase transitions observed in various DQC designer models, as well as their relation to specific quantum materials [23,24]. In view of these developments, it is crucial to establish quantum systems in which weakly first-order transitions can be robustly demonstrated and exact results for the properties at the transition point can be provided by insightful approaches.

Here, we uncover weakly first-order transitions in spin-one quantum magnets on the three-dimensional cubic lattice with SU(2) symmetric interactions. By large-scale quantum Monte Carlo (QMC) simulations, we establish that contrary to claims of a continuous transition [25], the planar spin-nematic (ferroquadrupolar) phase that emerges in this system melts across a weakly first-order transition (in contrast to fluctuation-induced first-order spin-nematic transitions in itinerant systems [26], the transition considered here is first order in mean-field theory [27]). Its discontinuous nature becomes apparent (in both the thermodynamic properties as well as the order parameter distribution) only on sufficiently large length scales, beyond those accessed previously [25]. In contrast to the case of the Potts model and designer models of DQC, in this system the weakly first-order transition takes place between a paramagnet and a low-temperature ordered phase that breaks a continuous internal SU(2) symmetry (certain classical models with continuous symmetries and strong nonlinear interactions have been shown rigorously to feature first-order transitions to nematic order [28–30]). Moreover, we show how calculations based on Poisson-Dirichlet distributions (PDs) within a universal loop model formulation of the spin-one lattice model can be used to derive the exact order parameter distribution in the quantum spin-nematic phase as well as order parameter Binder cumulants at the transition point, thereby providing us with a quantitative characterization of this weakly first-order thermal order-disorder transition. We note that the spin-one material $NiGa_2S_4$ is a candidate system for the planar spin-nematic state considered here [31–36].

Model and planar spin-nematic. To stabilize the planar spin-nematic state, we consider the generic SU(2)-symmetric spin-one Hamiltonian, i.e., with both bilinear and biquadratic interactions, on a simple cubic lattice Λ,

$$H = -J \sum_{\langle i,j\rangle \in \mathcal{B}_\Lambda} [u(\mathbf{S}_i \cdot \mathbf{S}_j) + v(\mathbf{S}_i \cdot \mathbf{S}_j)^2], \qquad (1)$$

with $|\Lambda| = L^3$ sites, and a sum over the (nearest-neighbor) bonds $\mathcal{B}_\Lambda$ of Λ (with periodic boundary conditions). It is convenient to fix $v = 1$ and keep u as a free parameter. Alternatively, an angular parametrization, $u = \cos(\phi)$, $v = \sin(\phi)$ can be used. In any case, we fix $J = 1$. For $u \in (0, 1)$ [i.e., $\phi \in (\pi/4, \pi/2)$], H harbors an extended planar spin-nematic phase [25,37–41], in which magnetic fluctuations are constrained to the plane perpendicular to a director $\vec{a} \in P\mathbb{S}^2$, the projective sphere, i.e., $\vec{a}$ is identified with $-\vec{a}$. Each director corresponds to an extremal Gibbs state $\langle\cdot\rangle_{\vec{a}}$ [41]. The symmetric Gibbs state at inverse temperature $\beta = 1/T$, $\langle\cdot\rangle_\beta = \mathrm{Tr}\cdot e^{-\beta H}/Z$, $Z = \mathrm{Tr} e^{-\beta H}$, in the infinite-volume limit, then has the decomposition [41] $\lim_{L\to\infty}\langle\cdot\rangle_\beta = \int_{P\mathbb{S}^2}\langle\cdot\rangle_{\vec{a}}\, d\vec{a}$. Here, $d\vec{a}$ denotes the uniform probability measure on $P\mathbb{S}^2$. In general, $\langle\cdot\rangle_{\vec{a}}$ depends on β (for small β the Gibbs state is unique and $\langle\cdot\rangle_{\vec{a}}$ does not depend on $\vec{a}$). A suitable local operator to detect nematic order is $Q_i = (S_i^z)^2 - \frac{2}{3}$, and we denote by n^* the "spontaneous nematization" in the z direction, $n^* = \langle Q_i\rangle_{\vec{e}_z}$, where i is any site. From the PD formulation introduced below, it follows that $n^* < 0$ [42]. In contrast to the axial nematic state that appears, e.g., for H with classical spins at $u = 0$ [43,44], the planar nematic phase is characterized by the *minimization* of the fluctuations in the plane perpendicular to the director, and $\langle\cdot\rangle_{\vec{a}} = \lim_{h\to 0+}\lim_{L\to\infty}\langle\cdot\rangle_{H+h\sum_{i\in\Lambda}(\vec{a}\cdot\vec{S}_i)^2}$ (notice the "+" sign in front of h) [41]. This is a genuine quantum mechanical phenomenon, related to the $m = 0$ state of the spin-one variables in this system. For $u = 0$ and $u = 1$, the model exhibits an enhanced SU(3) symmetry and ferromagnetic low-temperature order [41,45]. In the following, we study the properties of the model H at finite T, in particular the nature of the thermal melting of the spin-nematic state and its quantitative description.

Loop model and PD predictions. Loop models involve one-dimensional objects "living" in d-dimensional space. Phases may occur where loops of diverging lengths are present. It was recently observed in Ref. [46] that the joint distribution of the lengths of long loops displays universal behavior: It is always given by the stationary distribution of a split-merge process, which is PD characterized by a real number, the PD parameter θ (cf. Supplemental Material [42] for a basic introduction to PD and split-merge processes). We denote the corresponding distribution by PD(θ). It is possible to derive a loop model representation for H using the Trotter or Duhamel formulas for the Gibbs operator $\mathrm{e}^{-\beta H}$. It is restricted to $u \in [0, 1]$ (outside this domain, the representation involves negative weights). This combines representations due to Tóth [47] and to Aizenman and Nachtergaele [48] and was proposed in Ref. [45]. The latter paper contains a detailed derivation. The resulting representation is illustrated in Fig. 1. On top of each bond of the spatial lattice Λ is the "time" interval $[0, \beta]$. In each interval is an independent Poisson point process where "crosses" occur with intensity u and "double bars" occur with intensity $1 - u$. One then defines the loops as the closed trajectories obtained by moving vertically, and jumping on the neighboring site when encountering a cross or a double bar. If it is a cross, one continues in the same vertical direction, while if it is a double bar, one changes the vertical direction. The role of the loops is twofold: (i) They affect the probability of the loops because of a factor $3^{\#\mathrm{loops}}$, and (ii) quantum correlations are given by loop correlations. The relation between quantum spins and loops concerns the partition function via

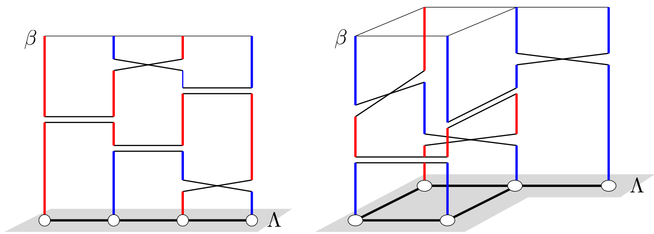

FIG. 1. Illustration of the loop model on different small lattices (for H, Λ is the cubic lattice).

$$Z = e^{2\beta|\mathcal{B}_\Lambda|}\sum_{k,\ell=0}^{\infty}\frac{\bar{u}^k u^\ell}{k!\,\ell!}\sum_{\substack{b_1,\ldots,b_k\\ c_1,\ldots,c_\ell}}\int_0^\beta ds_1\cdots ds_k dt_1\cdots dt_\ell\, 3^{|\mathcal{L}(\omega)|}.$$

Here, ω denotes a configuration in terms of $b_1, \ldots, b_k \in \mathcal{B}_\Lambda$ ($c_1, \ldots, c_\ell \in \mathcal{B}_\Lambda$), the bonds corresponding to double bars (crosses), and $s_1, \ldots, s_k \in [0, \beta]$ ($t_1, \ldots, t_\ell \in [0, \beta]$), the times at which double bars (crosses) occur. $\mathcal{L}(\omega)$ denotes the set of loops, and $\bar{u} = 1 - u$.

Furthermore, we obtain for the characteristic function of the "nematic histogram," i.e., the distribution function ρ_Q of the ferroquadrupolar operator $Q = \frac{1}{|\Lambda|}\sum_{i\in\Lambda} Q_i$ in the Gibbs state $\langle\cdot\rangle_\beta$, the identity (for any $k \in \mathbb{C}$)

$$\left\langle e^{ikQ}\right\rangle_\beta = \left\langle \prod_{\gamma\in\mathcal{L}(\omega)}\left(\frac{1}{3}e^{-\frac{2}{3}\frac{ik}{|\Lambda|}\ell(\gamma)} + \frac{2}{3}e^{\frac{1}{3}\frac{ik}{|\Lambda|}\ell(\gamma)}\right)\right\rangle_\beta^{\mathrm{loops}}, \qquad (2)$$

where the length $\ell(\gamma)$ of the loop γ is defined as the number of sites traversed by the loop at time 0, and $\langle\cdot\rangle_\beta^{\mathrm{loops}}$ denotes the expectation with respect to the loop measure above. This measure can be viewed as the invariant measure of a Markov process, involving the insertion and removal of double bars and crosses [41,49], as detailed in the Supplemental Material [42] (note that this process would be too slow to use in simulations.) Any new cross or double bar between two loops causes them to merge. When $u \in (0, 1)$, a subtle phenomenon occurs: A new cross or double bar may either cause a loop to split, or reorganize it without splitting it (this is akin to $0 \leftrightarrow 8$); either occurs with probability $\frac{1}{2}$. The lengths of macroscopic loops can be shown to satisfy an effective split-merge process, and the invariant distribution is PD(3/2) [46,50,51]. For $u = 0$ or $u = 1$, the subtle phenomenon above does not occur; splits then happen at twice the rate, and $\theta = 3$.

The PD conjecture [41,46] states that, as $L \to \infty$, we can replace the expectation in the loop model by the expectation with respect to PD(θ), scaled by a number $\eta = \eta(u, \beta) \in [0, 1]$ that represents the fraction of sites in long loops at imaginary time 0. This can be used to calculate the characteristic

TABLE I. PD results for the moments of Q.

	θ	$\langle Q^2\rangle_\beta$	$\langle Q^3\rangle_\beta$	$\langle Q^4\rangle_\beta$
$u \in (0, 1)$	3/2	$\frac{4}{45}\eta^2$	$-\frac{16}{27\cdot 35}\eta^3$	$\frac{16}{27\cdot 35}\eta^4$
$u \in \{0, 1\}$	3	$\frac{1}{18}\eta^2$	$-\frac{1}{135}\eta^3$	$\frac{1}{135}\eta^4$

function of ρ_Q explicitly [42]:

$$\lim_{L\to\infty}\langle e^{ikQ}\rangle_\beta = e^{-\frac{2}{3}ik\eta}\sum_{r=0}^{\infty}\frac{\Gamma\left(\frac{3}{2}\right)}{\Gamma\left(r+\frac{3}{2}\right)}(ik\eta)^r. \tag{3}$$

Inverse Fourier transform finally gives [42]

$$\rho_Q(s) = \begin{cases}\frac{1}{2\sqrt{\eta}\sqrt{\frac{1}{3}\eta - s}} & \text{if } -\frac{2}{3}\eta \leqslant s \leqslant \frac{1}{3}\eta,\\ 0 & \text{otherwise.}\end{cases} \tag{4}$$

From here, we can calculate the moments $\langle Q^n\rangle_\beta$ in the nematic phase. It is more insightful however, to derive them from the loop representation directly, using the PD conjecture to write them all in terms of the single unknown variable η. Cumulant ratios, such as $U_Q = 1 - \frac{1}{3}\langle Q^4\rangle_\beta/\langle Q^2\rangle_\beta^2$, are then given by ratios that no longer depend on η. We provide the calculations in some detail in the Supplemental Material [42]. The identities for the second, third, and fourth moment that are exact in the infinite-volume limit read

$$\begin{aligned}\langle Q^2\rangle_\beta &= \tfrac{2}{9}\mathbb{P}_\beta^{\text{loops}}[i_1, i_2 \text{ in same loop}],\\ \langle Q^3\rangle_\beta &= -\tfrac{2}{27}\mathbb{P}_\beta^{\text{loops}}[i_1, i_2, i_3 \text{ in same loop}],\\ \langle Q^4\rangle_\beta &= \tfrac{2}{27}\mathbb{P}_\beta^{\text{loops}}[i_1, i_2, i_3, i_4 \text{ in same loop}]\\ &\quad + \tfrac{4}{27}\mathbb{P}_\beta^{\text{loops}}[i_1, i_2 \text{ in same loop}, i_3, i_4 \text{ in other loop}].\end{aligned} \tag{5}$$

Here, i_1, i_2, i_3, and i_4 are sites that are very distant from one another. Since the sites are distant, it is necessary that they belong to long loops in order to have a chance to be in the same loop. We can then use the PD conjecture to obtain the probability $\mathbb{P}_\beta^{\text{loops}}[i_1, \ldots, i_n \text{ in same loop}]$, that $i_1, \ldots, i_n$ belong to the same loop, in terms of the probability that, if we choose a random partition of [0,1] according to PD(θ), and n-independent points in [0,1], all n points are in the same partition element [42]:

$$\begin{aligned}&\mathbb{P}_\beta^{\text{loops}}[i_1, \ldots, i_n \text{ in same loop}]\\ &\quad = \eta^n\mathbb{P}_{\text{PD}(\theta)}[n \text{ random points in same partition element}]\\ &\quad = \eta^n\frac{\Gamma(1+\theta)\Gamma(n)}{\Gamma(n+\theta)},\end{aligned}$$

and similarly

$$\begin{aligned}&\mathbb{P}_\beta^{\text{loops}}[i_1, i_2 \text{ in same loop}, i_3, i_4 \text{ in other loop}]\\ &\quad = 2\eta^4\sum_{k<\ell}\mathbb{P}_{\text{PD}(\theta)}[i_1, i_2 \text{ in } k\text{th element}, i_3, i_4 \text{ in } \ell\text{th el.}]\\ &\quad = 2\eta^4\frac{\theta\Gamma(1+\theta)}{\Gamma(4+\theta)}.\end{aligned}$$

The resulting moments are given in Table I. We obtain an η-independent value $U_Q^- = 2/7$ for the Binder cumulant in the thermodynamic limit within the planar spin-nematic phase, and η-independent values for the ratios of the moments toward the SU(3) end points, such as $\lim_{u\to 0^+}\langle Q^2\rangle_\beta(u)/\langle Q^2\rangle_\beta(u = 0) = \lim_{u\to 1^-}\langle Q^2\rangle_\beta(u)/\langle Q^2\rangle_\beta(u = 1) = 8/5$. The moments of Q can also be calculated using symmetry breaking extremal states [42], for which, however, the heuristics is more subtle and the result may be uncertain.

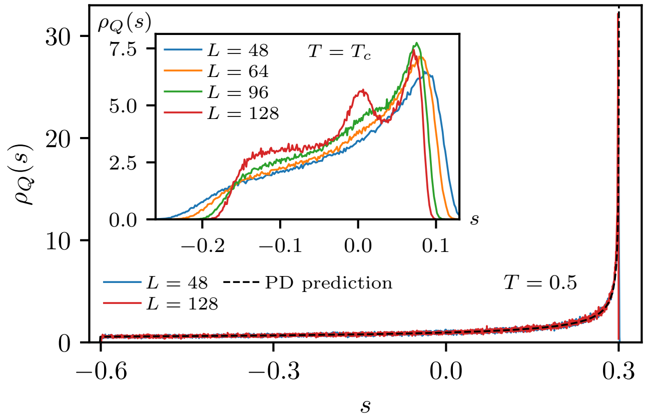

FIG. 2. Comparison of the nematic histogram obtained from QMC at $u = \cot(3\pi/8)$ with the PD prediction for $\eta = 0.9021(2)$. The inset shows the histogram for various L at the transition temperature $T_c = 1.649\,00(1)$.

Comparison to QMC. We verify the above results, obtained from the PD conjecture, by making use of unbiased large-scale QMC simulations, based on the stochastic series expansion [52,53]. Figure 2 compares the PD prediction for ρ_Q with the nematic histogram obtained using QMC simulations for $u = \cot(\phi = 3\pi/8) = 0.414\,12\ldots$, i.e., at the center of the spin-nematic regime in the angular parametrization of H, at a low temperature of $T = 0.5$ in the ordered phase (similar results are obtained for other values of u). We observe a remarkable agreement between the nematic histogram and the PD prediction. In Fig. 3, we show the thermal evolution of U_Q

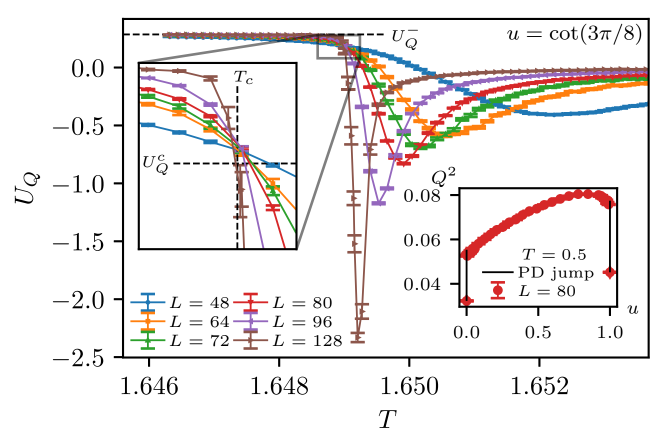

FIG. 3. Temperature dependence of the Binder cumulant U_Q near the phase transition for different system sizes at $u = \cot(3\pi/8)$ from QMC. The PD-based predictions U_Q^- in the ordered phase and U_Q^c at the transition temperature T_c are indicated by dashed lines. The right inset shows the u dependence of the second moment $\langle Q^2\rangle_\beta$.

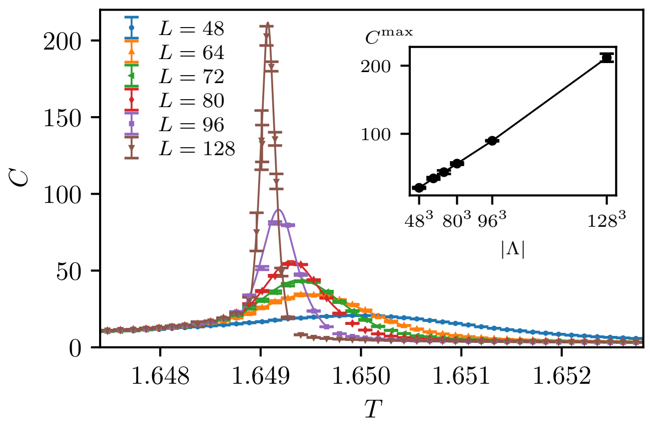

FIG. 4. Temperature dependence of the specific heat C for different system sizes at $u = \cot(3\pi/8)$ from QMC. The inset shows the scaling of the maximum $C^{\max}$ with system size, extracted from the shown Lorentzian interpolations.

and find that within the ordered phase, the QMC data converge toward the PD prediction upon increasing the system size (U_Q converges to 0 in the paramagnetic regime). We also examine in the inset of Fig. 3 the u evolution of $\langle Q^2\rangle_\beta$ at a fixed low temperature $T = 0.5$. We observe an explicit u dependence of the second moment (reflected by the u dependence of η in the PD prediction), as well as the agreement in the relative size of its jump to both SU(3) end points with the PD prediction.

Next, we consider the phase transition. We demonstrate that in contrast to earlier claims, the planar spin-nematic order melts across a (weakly) first-order thermal transition. A basic quantity for this purpose is the specific heat C, the T dependence of which is shown in Fig. 4. For sufficiently large systems, we clearly identify a prominent peak with a scaling $C^{\max} \propto |\Lambda|$, characteristic of a first-order transition. From an extrapolation of the peak position [42], we obtain the estimate $T_c = 1.649\,00(1)$ for the transition temperature at this parameter value.

Further evidence for the first-order character of the transition is obtained from considering the nematic histogram at T_c. This is shown in the inset of Fig. 2, and exhibits the coexistence of two contributions: (i) a broad low-T contribution akin to the one in the main panel, and (ii) a further, comparably sharp peak near $Q = 0$, i.e., related to disordered states. The latter emerges only mildly upon increasing the system size, but it is clearly resolved for $L \gtrsim 100$. This indicates the rather weak first-order character of the transition. Histograms based on the internal energy also support this conclusion [42]. Another quantity that exhibits genuine behavior at first-order transitions is the Binder cumulant U_Q, shown in Fig. 3 across the transition region. Two properties are noticeable: (i) U_Q develops a substantial dip just above T_c, which grows and sharpens with increasing L, another characteristic feature of first-order transitions [54]. (ii) The data for U_Q from different system sizes exhibit a crossing at T_c. We can calculate the crossing point value U_Q^c as follows from considering the coexistence of ordered and disordered states: Denoting by α the weight of the ordered states at coexistence, such that $\langle\cdot\rangle_{\beta_c} = \alpha \lim_{\beta\to\beta_c^+}\langle\cdot\rangle_\beta + (1-\alpha)\lim_{\beta\to\beta_c^-}\langle\cdot\rangle_\beta$, we can express U_Q^c in terms of the previously calculated moments of Q in the nematic phase, taking into account that they vanish in the paramagnetic phase. This gives $U_Q^c = 1 - 5/(7\alpha)$. We finally need to determine the mixing parameter α at the first-order transition in the quantum system described by H. A related issue appears for first-order transitions in *classical* models with continuous variables, and this has been addressed only recently [55]: Based on the fact that for the discrete q-state Potts model the corresponding parameter is given in terms of the number q of distinct degenerate low-T sectors with respect to the single paramagnetic sector by $\alpha = q/(q+1)$, it was argued that for the continuous case, α is obtained upon replacing q in the above formula by the integral measure of the space of extremal states. In the current case this measure is given by the area 2π of the projective sphere $P\mathbb{S}^2$, i.e., $\alpha = 2\pi/(2\pi+1)$. The value of $U_Q^c = 2/7 - 5/(14\pi) = 0.1720\ldots$ resulting from this heuristics indeed matches remarkably well to the QMC data (cf. the inset in Fig. 3). This demonstrates that PD calculations provide an accurate quantitative description of the planar spin-nematic phase of the spin-one quantum magnet. It would be valuable to base the heuristics of Ref. [55] on more rigorous considerations for both continuous and quantum variables.

Conclusions. We used a combination of QMC and PD calculations, based on a loop model formulation, to uncover weakly first-order thermal melting transitions of planar spin-nematic states realized in quantum spin-one systems with SU(2)-symmetric interactions. We demonstrated explicitly how generic properties of both the low-temperature nematic phase and the phase coexistence line can be calculated based on the PD conjecture, with remarkable agreement to QMC results. Further studies, e.g., based on RG approaches, will be useful in order to explain the weakness of these transitions via the tuning mechanism, or by connecting it to the ideas of walking and fixed-point annihilation within this well-defined framework of a comparably simple quantum spin model.

Acknowledgments. We thank A. Honecker, J. B. Hauck, and P. Sengupta for insightful discussions. We acknowledge support by the Deutsche Forschungsgemeinschaft (DFG) through Grant No. WE/3649/4-2 of the FOR 1807 and RTG 1995, and thank the IT Center at RWTH Aachen University and JSC Jülich for access to computing time through JARA CSD.

[1] D. B. Kaplan, J.-W. Lee, D. T. Son, and M. A. Stephanov, Phys. Rev. D **80**, 125005 (2009).

[2] A. Nahum, J. T. Chalker, P. Serna, M. Ortuño, and A. M. Somoza, Phys. Rev. X **5**, 041048 (2015).

[3] C. Wang, A. Nahum, M. A. Metlitski, C. Xu, and T. Senthil, Phys. Rev. X **7**, 031051 (2017).

[4] V. Gorbenko, S. Rychkov, and B. Zan, J. High Energy Phys. 10 (2018) 108.

[5] V. Gorbenko, S. Rychkov, and B. Zan, SciPost Phys. **5**, 050 (2018).
[6] H. Ma and Y.-C. He, Phys. Rev. B **99**, 195130 (2019).
[7] F. S. Nogueira, J. van den Brink, and A. Sudbø, Phys. Rev. D **100**, 085005 (2019).
[8] S. Iino, S. Morita, N. Kawashima, and A. W. Sandvik, J. Phys. Soc. Jpn. **88**, 034006 (2019).
[9] J. D'Emidio, A. A. Eberharter, and A. M. Läuchli, arXiv:2106.15462.
[10] F. Y. Wu, Rev. Mod. Phys. **54**, 235 (1982).
[11] M. Nauenberg and D. J. Scalapino, Phys. Rev. Lett. **44**, 837 (1980).
[12] J. L. Cardy, M. Nauenberg, and D. J. Scalapino, Phys. Rev. B **22**, 2560 (1980).
[13] B. Holdom, Phys. Rev. D **24**, 1441 (1981).
[14] K. Yamawaki, M. Bando, and K.-i. Matumoto, Phys. Rev. Lett. **56**, 1335 (1986).
[15] T. Appelquist, D. Karabali, and L. C. R. Wijewardhana, Phys. Rev. Lett. **57**, 957 (1986).
[16] T. Senthil, A. Vishwanath, L. Balents, S. Sachdev, and M. P. A. Fisher, Science **303**, 1490 (2004).
[17] A. W. Sandvik, Phys. Rev. Lett. **98**, 227202 (2007).
[18] T. Senthil, L. Balents, S. Sachdev, A. Vishwanath, and M. P. A. Fisher, Phys. Rev. B **70**, 144407 (2004).
[19] H. Shao, W. Guo, and A. W. Sandvik, Science **352**, 213 (2016).
[20] N. Ma, G.-Y. Sun, Y.-Z. You, C. Xu, A. Vishwanath, A. W. Sandvik, and Z. Y. Meng, Phys. Rev. B **98**, 174421 (2018).
[21] R. Ma and C. Wang, Phys. Rev. B **102**, 020407(R) (2020).
[22] A. Nahum, Phys. Rev. B **102**, 201116(R) (2020).
[23] J. Yang, A. W. Sandvik, and L. Wang, Phys. Rev. B **105**, L060409 (2022).
[24] Y. Cui, L. Liu, H. Lin, K.-H. Wu, W. Hong, X. Liu, C. Li, Z. Hu, N. Xi, S. Li, R. Yu, A. W. Sandvik, and W. Yu, arXiv:2204.08133.
[25] K. Harada and N. Kawashima, Phys. Rev. B **65**, 052403 (2002).
[26] T. R. Kirkpatrick and D. Belitz, Phys. Rev. Lett. **106**, 105701 (2011).
[27] H. H. Chen and P. M. Levy, Phys. Rev. B **7**, 4267 (1973).
[28] A. C. D. van Enter and S. B. Shlosman, Commun. Math. Phys. **255**, 21 (2005).
[29] A. Messager and B. Nachtergaele, J. Stat. Phys. **122**, 1 (2006).
[30] M. Biskup and R. Kotecký, Commun. Math. Phys. **264**, 631 (2006).
[31] S. Nakatsuji, Y. Nambu, H. Tonomura, O. Sakai, S. Jonas, C. Broholm, H. Tsunetsugu, Y. Qiu, and Y. Maeno, Science **309**, 1697 (2005).
[32] Y. Nambu, S. Nakatsuji, and Y. Maeno, J. Phys. Soc. Jpn. **75**, 043711 (2006).
[33] H. Tsunetsugu and M. Arikawa, J. Phys. Soc. Jpn. **75**, 083701 (2006).
[34] A. Läuchli, F. Mila, and K. Penc, Phys. Rev. Lett. **97**, 087205 (2006).
[35] S. Bhattacharjee, V. B. Shenoy, and T. Senthil, Phys. Rev. B **74**, 092406 (2006).
[36] M. E. Valentine, T. Higo, Y. Nambu, D. Chaudhuri, J. Wen, C. Broholm, S. Nakatsuji, and N. Drichko, Phys. Rev. Lett. **125**, 197201 (2020).
[37] K. Tanaka, A. Tanaka, and T. Idogaki, J. Phys. A: Math. Gen. **34**, 8767 (2001).
[38] C. D. Batista and G. Ortiz, Adv. Phys. **53**, 1 (2004).
[39] T. A. Tóth, A. M. Läuchli, F. Mila, and K. Penc, Phys. Rev. B **85**, 140403(R) (2012).
[40] Y. Fridman, O. Kosmachev, and P. Klevets, J. Magn. Magn. Mater. **325**, 125 (2013).
[41] D. Ueltschi, Phys. Rev. E **91**, 042132 (2015).
[42] See Supplemental Material at http://link.aps.org/supplemental/10.1103/PhysRevB.107.L020409 for (i) an introduction to PD and split-merge processes, (ii) the identification of the PD parameter, (iii) the PD calculation of the nematic histogram, (iv) the symmetry breaking calculations of the nematic histogram, (v) the calculation of the Binder cumulants, (vi) the energy histograms from QMC, and (vii) the determination of T_c, which includes Refs. [56–61].
[43] N. Angelescu and V. A. Zagrebnov, J. Phys. A: Math. Gen. **15**, L639 (1982).
[44] M. Biskup and L. Chayes, J. Phys. A: Math. Gen. **238**, 53 (2003).
[45] D. Ueltschi, J. Math. Phys. **54**, 083301 (2013).
[46] C. Goldschmidt, D. Ueltschi, and P. Windridge, in *Entropy and the Quantum II*, edited by R. Sims and D. Ueltschi, Contemporary Mathematics (American Mathematical Society, Providence, RI, 2011), Vol. 552, pp. 177–224.
[47] B. Tóth, Lett. Math. Phys. **28**, 75 (1993).
[48] M. Aizenman and B. Nachtergaele, Commun. Math. Phys. **164**, 17 (1994).
[49] D. Ueltschi, Universal behaviour of 3D loop soup models, in *6th Warsaw School of Statistical Physics*, edited by B. Cichocki, M. Napiorkowski, J. Piasecki, and P. Szymczak (Warsaw University Press, Warsaw, Poland, 2017), pp. 65–100.
[50] N. V. Tsilevich, Theory Probab. Appl. **44**, 60 (2000) .
[51] P. Diaconis, E. Mayer-Wolf, O. Zeitouni, and M. P. W. Zerner, Ann. Probab. **32**, 915 (2004).
[52] A. W. Sandvik, Phys. Rev. B **59**, R14157 (1999).
[53] O. F. Syljuåsen and A. W. Sandvik, Phys. Rev. E **66**, 046701 (2002).
[54] K. Binder, Rep. Prog. Phys. **50**, 783 (1987).
[55] J. Xu, S.-H. Tsai, D. P. Landau, and K. Binder, Phys. Rev. E **99**, 023309 (2019).
[56] A. Nahum, J. T. Chalker, P. Serna, M. Ortuño, and A. M. Somoza, Phys. Rev. Lett. **111**, 100601 (2013).
[57] S. Grosskinsky, A. A. Lovisolo, and D. Ueltschi, J. Stat. Phys. **146**, 1105 (2012).
[58] A. M. Ferrenberg and R. H. Swendsen, Phys. Rev. Lett. **61**, 2635 (1988).
[59] J. Lee and J. M. Kosterlitz, Phys. Rev. Lett. **65**, 137 (1990).
[60] J. Lee and J. M. Kosterlitz, Phys. Rev. B **43**, 3265 (1991).
[61] W. Janke, Phys. Rev. B **47**, 14757 (1993).